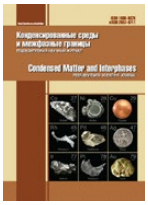

ISSN 1606-867X (Print)
ISSN 2687-0711 (Online)
Condensed Matter and Interphases
Kondensirovannye Sredy i Mezhfaznye Granitsy
https://journals.vsu.ru/kcmf/

Original articles

Research article
https://doi.org/10.17308/kcmf.2025.27/13016

Mechanical properties of Li-Nb-O system films

A. V. Kostyuchenko[1]✉, E. K. Belonogov[1,2], V. M. Ievlev[1,2,3], A. E. Nikonov[1], E. A. Osipov[1], P. A. Osipov[1]

[1]Voronezh State Technical University,
20 let Oktyabrya st., 84, Voronezh 394006, Russian Federation

[2]Voronezh State University,
1, University pl., Voronezh 394018, Russian Federation

[3]Moscow State University,
1, Leninskie Gory, Moscow 119991, Russian Federation

Abstract

Objective: To quantitatively assess the hardness, elasticity, and plasticity of Li-Nb-O system films and to determine the influence of the structure and substructure on these parameters in them.

Experimental: Li-Nb-O system films with a thickness of ~0.8 μm were grown on non-heated substrates (oxidized single-crystal silicon wafers (SiO_2 layer ~0.4 μm), single-crystal lithium niobate with (0001) orientation) by ion beam sputtering of a lithium niobate target. Thermal annealing of Li-Nb-O films on substrates was performed in air for 10 min (until complete crystallization) at temperatures of 550, 650, 700, 750, 800, and 850 °C. The heterostructures (film/substrate) were cooled with a furnace. The phase composition of the films was investigated by X-ray diffraction (XRD) and selected area electron diffraction (SAED). The substructure was studied by transmission electron microscopy (TEM) and high-resolution TEM (HRTEM, Tecnai G2 30ST) of cross-sectional specimens prepared by ion milling using a Quanta 3D setup. The surface morphology was investigated by scanning electron microscopy (SEM, Teskan Mira) in the topological contrast mode and atomic force microscopy (AFM, Solver47). The mechanical properties, hardness (H) and Young's modulus (E), were determined from nanoindentation (NI, NanoHardness Tester CSM Instruments) measurements using a Berkovich diamond indenter under the following conditions: maximum load 10 mN, loading rate 10 mN/min, and unloading rate 15 mN/min.

Results: It was found that thermal annealing in an oxygen-containing atmosphere at 750°C induces the crystallization of quasi-amorphous Li-Nb-O films and the synthesis of single-phase LN films with lattice parameters closest to those of stoichiometric single-crystal LN. The most probable mechanisms of irreversible deformation in LN films are: brittle fractures, plastic deformation of crystallites, and grain boundary sliding. LN films synthesized at 650-750°C are most susceptible to brittle fracture. Brittle fractures occur due to the buildup of macrostresses in the films, resulting from different coefficients of thermal expansion (CTE) of the film and the substrate. The fracture toughness of the films increases significantly when using a substrate with a CTE close to that of the film. The hardness of nano- and microcrystalline LN films is always higher than the hardness of quasi-amorphous Li-Nb-O system films. The decrease in the hardness of films synthesized at high annealing temperatures is due to a decrease in the concentration of point defects and an increase in the size of the crystallites.

Keywords: Thin film, Lithium niobate, Thermal annealing, Crystallization, Structure, Surface morphology, Nanoindentation, Hardness, Cracking

Funding: The study was financially supported by the Russian Science Foundation as part of scientific project No. 24-22-20046.

***Acknowledgments*:** Scanning electron microscopy studies were performed using equipment at the Basic Scientific and Educational Center "Physics and Technology of Thermoelectric Phenomena" of Voronezh State Technical University.

For citation: Kostyuchenko A. V., Belonogov E. K., Ievlev V. M., Nikonov A. E., Osipov E. A., Osipov P. A. Mechanical properties of Li-Nb-O films. *Condensed Matter and Interphases*. 2025;27(3): 398–408. https://doi.org/10.17308/kcmf.2025.27/13016

✉ Alexander V. Kostyuchenko, e-mail: av-kostuchenko@mail.ru

Для цитирования: Костюченко А. В., Белоногов Е. К., Иевлев В. М., Никонов А. Е., Осипов Е. А., Осипов П. А. Механические свойства пленок системы Li-Nb-O. *Конденсированные среды и межфазные границы*. 2025;27(3): 398–408. https://doi.org/10.17308/kcmf.2025.27/13016

1. Introduction

To realize the potential of lithium niobate (LN, $LiNbO_3$) thin films as a functional material in optoelectronic [1], acoustoelectronic [2], and memory devices [3], it is necessary to develop an understanding of the deformation mechanism, mechanical properties, and prospects for bringing the functional parameters of thin films closer to those of single-crystal LN. Elastic properties, hardness, plasticity, surface morphology, and macro- and microstresses in the near-surface layer of LN films significantly affect electrical conductivity, sound velocity, acoustic wave attenuation [4, 5], electromechanical conversion efficiency, and optical transmittance [6, 7]. A large number of studies have been devoted to the regularities of LN film growth on substrates, as well as structural and substructural transformations in LN films as a result of various influences, in particular, thermal processing [8, 9, 10]. There are several works devoted to the study of the mechanical properties of LN single crystals. For example, in [11], nanoindentation results established that the hardness (H) and Young's modulus (E) of single-crystal LN wafers are ~12 and 194 GPa, respectively, for the X-cut, and 13 and 211 GPa for the Z-cut. In [12, 13], transmission electron microscopy (TEM) was used to observe dislocations in LN single crystals deformed at high temperatures, showing the dislocation mechanism of plastic deformation of LN. There are isolated works concerning the influence of thermal stresses on the structure and substructure of LN films. In particular, the dislocation mechanism of macrostress relaxation in epitaxial heterostructures with large mismatch in composition, structure, and thermal stresses arising from different coefficients of thermal expansion was established by the authors of [14] and [15]. In [16], the change in the lattice parameters of epitaxial LN films on sapphire as a result of thermal stresses is considered. At the same time, there is practically no data on the dependence of mechanical properties (hardness, Young's modulus, contribution of elastic and plastic components to deformation) of Li-Nb-O system films on structure, phase composition, and substructure; there is no systematic data necessary to identify the mechanism of stress relaxation in Li-Nb-O system films arising during synthesis and subsequent thermal processing.

The purpose of this work is to quantitatively assess the hardness, elasticity, and plasticity, and to determine the influence of structure and substructure on these parameters in Li-Nb-O system films.

2. Experimental

Li-Nb-O system films with a thickness of ~0.8 μm were grown on non-heated substrates (oxidized single-crystal silicon wafers (SiO_2 layer ~0.4 μm) and single-crystal lithium niobate with (0001) orientation) by ion beam sputtering of a lithium niobate target. Sputtering conditions: working gas – argon; ion beam current 90 mA; ion source electrode voltage 2.2 kV; a compensator system eliminates the shielding potential on the substrate. The distance from the target to the substrate during deposition was 10 cm.

Thermal annealing (TA) of Li-Nb-O/SiO_2/Si heterostructures was performed in air in a coaxial furnace for 10 min (until complete crystallization) at temperatures of 550, 650, 700, 750, 800, and 850 °C. Samples were loaded into the heated furnace. The heterostructures were left to cool in the furnace at a cooling rate of 300 °C/h.

The phase composition of the films was investigated by X-ray diffraction (XRD) using a Bruker D2 Phaser diffractometer (copper tube radiation) and selected area electron diffraction (SAED) using an EG-100M electron diffraction camera. The substructure was studied by transmission electron microscopy (TEM) and high-resolution TEM (HRTEM, Tecnai G2 30ST) of cross-sectional specimens prepared by ion milling using a Quanta 3D setup. The surface morphology was investigated by scanning electron microscopy (SEM, Teskan Mira) in topological contrast mode and atomic force microscopy (AFM, Solver47). The mechanical properties, hardness (H) and Young's modulus (E), were determined from nanoindentation (NI, NanoHardness Tester CSM

Instruments) measurements using a Berkovich diamond indenter under the following conditions: maximum load 10 mN, loading rate 10 mN/min, and unloading rate 15 mN/min.

3. Results and discussion

Phase Composition. According to XRD data (Fig. 1, diffractogram 1), the Li-Nb-O system films after deposition were X-ray amorphous or quasi-amorphous, in accordance with the terminology previously adopted in [17]. After isochronal annealing (Fig. 1, diffractograms 2–4), single-phase LN films crystallized (Fig. 1, curves 2, 3, 4). The single-phase composition of LN films was maintained throughout the used range of crystallization annealing temperatures. Profile analysis (Rietveld method) of XRD diffraction peaks showed an increase in the LN lattice parameters *a* and *c* with increasing annealing temperature (Table 1). The relative increase in the parameters was ~0.5%, which corresponds to a relative change in the volume of the unit cell of the crystal lattice by 1.1% with a method error of less than 0.1%. The significant increase in the lattice parameters was the result of oxygen diffusion into the LN lattice and a decrease in the concentration of oxygen vacancies. It follows from Table 1 that after thermal annealing at 750 °C and above, the volume of the crystal lattice was closest to the lattice volume of single-crystal

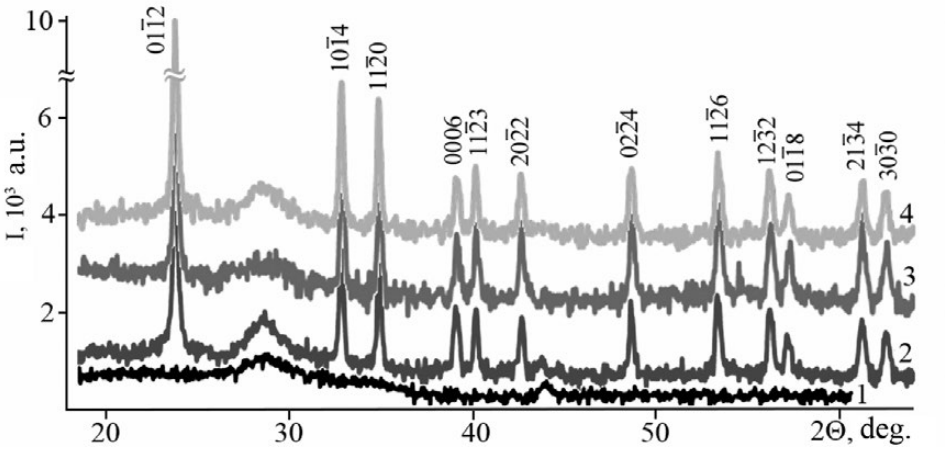

Fig. 1. X-ray diffraction of the Li-Nb-O/SiO_2 heterostructure before (*1*) and after annealing at temperatures of 550 (*2*), 750 (*3*), and 850 °C (*4*)

Table 1. Lattice parameters of lithium niobate for single crystal and polycrystalline films on the surface of oxidized silicon and single crystal LN orientation (0001) after TA at different temperatures (°C) of annealing

Substrate	TA, °C	*a*, Å	*c*, Å	$(V\text{-}V_0)/V_0$, %
(001) Si/SiO_2	550	5.132	13.775	–1.3
	650	5.142	13.805	– 0.7
	700	5.144	13.819	– 0.5
	750	5.151	13.835	– 0.1
	800	5.159	13.842	0.2
	850	5.156	13.843	0.1
(0001) LN	550	5.1316	13.785	–1.2
	650	5.1314	13.795	–1.2
	750	5.1328	13.798	–1.1
	800	5.1362	13.798	–1.0
	850	5.1395	13.799	–0.8

V – available lattice volume
V_0 – lattice volume of single-crystal LN [18]
Lattice parameters of single-crystal LN: *a* = 5.149 Å, *c* = 13.862 Å [18]

LN [18], which indicates a chemical composition closest to stoichiometric LN. An estimate of the average size of LN crystallites on the surface of oxidized silicon by the Scherrer method showed their growth from 25 to 75 nm throughout the entire range of annealing temperatures (Table 2). The most significant increase in crystallite size was observed during annealing at 850 °C (from 25 to 75 nm). The highest rate of crystallite growth (i.e., the change in size per degree) was observed in the temperature range from 550 to 650 °C. With a fixed annealing time, the observed evolution of the film structure with increasing temperature is probably associated with the sequential activation of various grain growth mechanisms. Thus, the rapid growth of crystallites in the range up to 650 °C may be due to collective recrystallization, while the additional increase in their size at 800 and 850 °C is likely associated with secondary recrystallization.

To assess the change in lattice parameters under conditions of minimal macrostresses, the crystal lattice of lithium niobate films obtained on a single-crystal LN was investigated. Fig. 2 shows XRD patterns of films obtained on the surface of (0001) LN single crystal. The diffractogram shows a complete set of maxima corresponding to the LN lattice. The observed increased intensity of the 0006 reflection indicates the formation of an axial texture <0001> LN. In films after TA at 750 °C, the intensity of the 0006 reflection was maximal. A further increase in TA temperature

Table 2. Average grain size of LN after TA

Temperature TA, °C	550	650	700	750	800	850
Average grain size, nm	24	47	51	54	64	73

led to a decrease in the reflection intensity. The increase in the degree of texturing of the films was probably due to the influence of the substrate on the selective growth of grains oriented along the [0001] axis during the coalescence recrystallization stage. During the stage of secondary recrystallization, the relative proportion of oriented grains decreased. According to the profile analysis of diffraction peaks, the *a* and *c* lattice parameters of LN increased by 0.2% with increasing TA temperature from 550 to 850 °C. As in the case of films on the surface of oxidized silicon, the increase in lattice parameters was the result of oxygen diffusion into the LN lattice during TA. The smaller change in parameters compared to films on oxidized silicon can be explained by the absence of macrostresses associated with the difference in the coefficients of thermal expansion of the film and the substrate.

Fig. 3 shows TEM images and an SAED pattern of an ultrathin cross-section of an Li-Nb-O system film before annealing. There is no contrast on the TEM image (Fig. 3a) characteristic of regions of coherent scattering. On the HRTEM image (Fig. 3b), the contrast has a stochastic character. On the electron diffraction patterns obtained by the SAED method from various regions of the

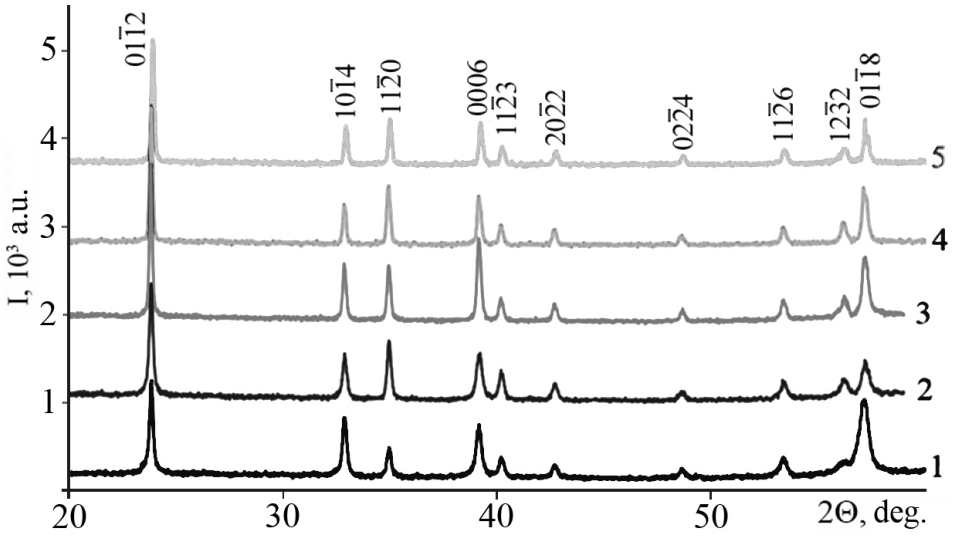

Fig. 2. X-ray diffraction of the Li-Nb-O/(0001)LN heterostructure after annealing at temperatures of 550 (*1*), 650 (*2*), 750 (*3*), 800 (*4*), and 850 °C (*5*)

film, there is always a characteristic halo (see inset in Fig. 3), indicating a quasi-amorphous structure of the initial Li-Nb-O system films. Figure 4 shows TEM images and an SAED pattern of an ultrathin cross-section of an Li-Nb-O system film after annealing at 550 °C. Regions of coherent scattering are clearly visible on the TEM image (Fig. 4a); the film has a nanocrystalline structure, with an average crystallite size of 40 nm. The HRTEM image (Fig. 4b) is dominated by a characteristic banded contrast with a period of 0.37 nm, corresponding to the period of the atomic planes (10 4) of the LN crystal lattice. Analysis of the electron diffraction pattern (inset in Fig. 4) also revealed a set of interplanar spacings characteristic of the LN lattice.

Surface Morphology. According to SEM data, an increase in the size of morphological inhomogeneities on the surface of the films as a result of increasing TA temperature correlates with a change in the size of the crystallites, as established by TEM and XRD results (Fig. 6). Cracks were observed in all films on SiO_2/Si substrates after annealing. Their formation is caused by macrostresses – a consequence of different coefficients of thermal expansion (CTE) of the film and the substrate: for silicon, the CTE is 5.1, and for LN it ranges from 5 to $15 \cdot 10^{-6}$ °C^{-1} in the [10 0] and [0001] directions, respectively. Figures 5a and b show AFM images of the surface of LN films on the surface of oxidized silicon after TA at 550 and 800 °C. Table 3 contains parameters obtained by AFM hardware, characterizing the surface relief of quasi-amorphous (Li-Nb-O) and crystalline LN films on the surface of SiO_2/Si. In films after annealing at 550 °C (Fig. 5a), the lateral dimensions of the relief inhomogeneities were 100 nm or more, and their height did not

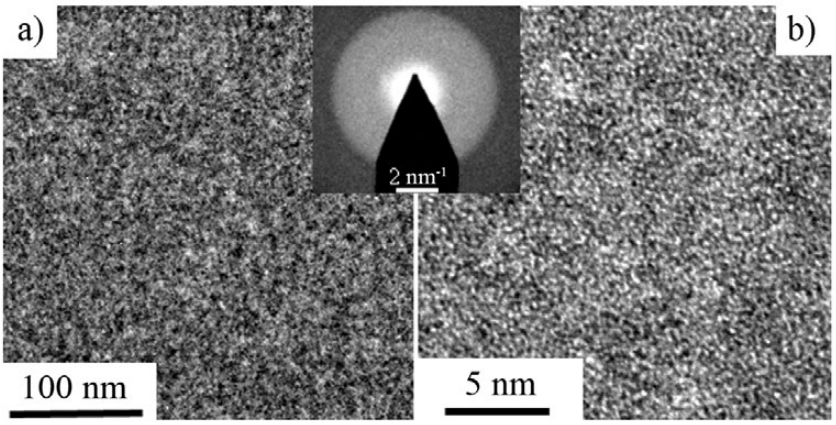

Fig. 3. TEM (a) and HRTEM (b) cross-section images of the Li-Nb-O film after deposition; inset shows a fragment of HEED

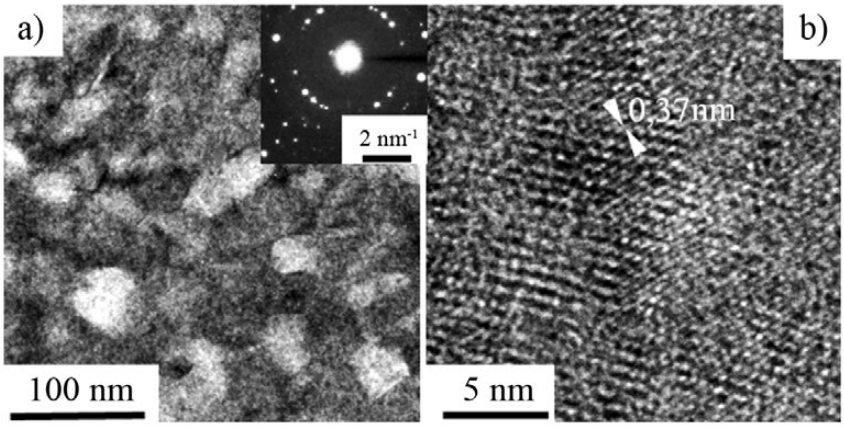

Fig. 4. TEM (a) and HRTEM (b) images of a cross-section of a Li-Nb-O film after annealing at 550 °C and a fragment of a HEED microelectron diffraction pattern

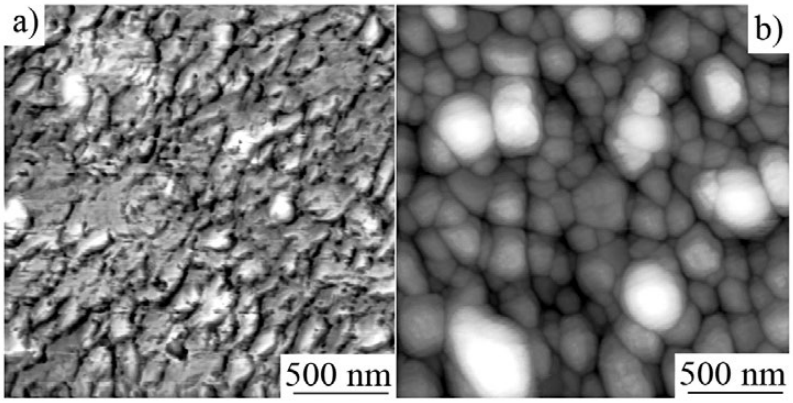

Fig. 5. AFM images of the surface of films annealed at 550 (a) and 800 °C (b) on the surface of SiO_2/Si substrates

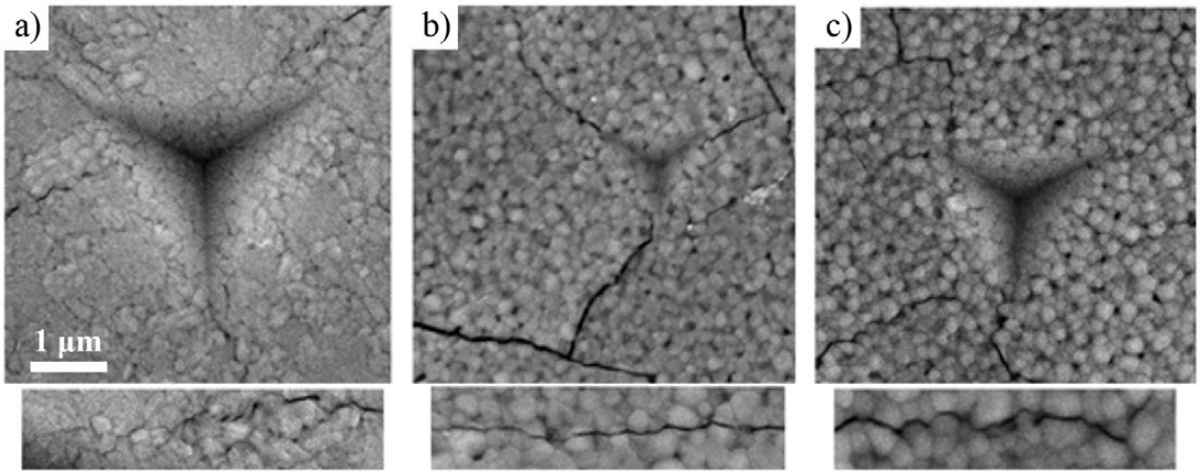

Fig. 6. SEM images of indenter imprints on the surface of films grown on SiO_2/Si and annealed at 550 (a), 750 (b), and 800 °C (c) with an indenter load of 10, 1, and 10 mN, respectively

Table 3. Relief parameters of lithium niobate films on the surface of oxidized silicon before and after thermal annealing

Relief parameters	without annealing	550 °C	750 °C	800 °C
Height difference, nm	20	55	110	120
Average roughness, nm	4	15	20	20

exceed 50 nm, i.e., the film relief was markedly flat. After annealing at 800 °C (see Fig. 5b), the most probable lateral dimensions of the inhomogeneities were ~ 150 nm, their height was ~170 nm, and the roughness was 20 nm; therefore, the film relief reflects the dispersity of the crystallites. The most significant changes in the relief were observed with increasing crystallization temperature. The development of the relief occured due to an increase in protrusions (presumably, crystallites). After crystallization of quasi-amorphous films, their roughness increased sharply. The roughness of films crystallized at 650–850 °C was practically unchanged (~ 20 nm), and the relief height difference was invariably higher in films crystallized at higher temperatures. That is, the development of the relief occured due to the selective growth of individual crystallites, but their volume fraction in the film is small. Morphological inhomogeneities after thermal annealing at 550 and 800 °C indicated, respectively, the nano- and microcrystalline structure of Li-Nb-O films.

Fig. 6 shows SEM images of indenter imprints that appeared on the surface of the film on SiO_2/Si substrates as a result of the applied loads. The sizes of morphological inhomogeneities of the surface relief of the films after thermal

annealing correlate with the results of the study using AFM. In addition to cracks that occurred immediately after thermal annealing, additional cracks appear near the imprints after NI (Fig. 6). The minimum load on the indenter that can cause additional cracking of films annealed at 750 °C was 1 mN (Fig. 6b). The cracking of films annealed at other temperatures was observed only at higher loads on the indenter (> 1 mN). If the load on the indenter was > 10 mN, then the NI process initiated cracking of the film regardless of the annealing temperature (Fig. 6a, c). The nature of crack propagation in the films was different: 1) in films after annealing at 550 °C, as a rule, the cracks propagated along the grain boundaries; 2) after annealing at 750 °C they mainly propagated through the volume of grains; 3) after 800 °C they mainly propagated along the grain boundaries (insets in Fig. 6).

Fig. 7 shows SEM images of indenter imprints on films on the surface of (0001) LN single crystal after TA at 750 and 800 °C. Cracks in the films were not observed. Comparing the obtained result with the result for films on oxidized silicon, it can be argued that the nature of crack formation in lithium niobate films is primarily associated with macrostresses caused by the difference in CTEs of the film and the substrate.

Elastic Modulus and Hardness. The mechanical properties of the films after thermal annealing at different temperatures were studied by NI. Table 4 presents the results of measuring the hardness (H), Young›s modulus (E), and the proportion of elastic deformation in the indentation work (η) of films and single-crystal lithium niobate at a load on the indenter up to 1 mN. Fig. 8 shows P-h diagrams for annealed films and the surface of (0001) LN single crystal obtained by NI when the load on the indenter increased to 10 mN. The P-h diagrams of all samples, including the single crystal, have steps (highlighted in Fig. 8). Moreover, with increasing film annealing temperature, the minimum load for their appearance decreased.

According to [11], the hardness and Young's modulus of bulk single-crystal LN for the X-cut are 11.8 and 194 GPa, respectively. The experimental values of hardness and elastic moduli of Z-cuts of single crystals after technological machining are slightly lower (Table 4).

The hardness of quasi-amorphous Li-Nb-O films is lower than the hardness of nano- and microcrystalline LN films. Considering the low probability of implementing a dislocation mechanism of plastic deformation in such films and the absence of cracks in them, the most probable mechanism of plastic deformation is the movement of elementary structural clusters according to the mechanism described in [19] for hydroxyapatite ceramics and films. The hardness and elasticity of crystalline LN films on the SiO_2/Si surface also did not reach the values characteristic of a single crystal. A notable feature for the films is the decrease in the hardness of films annealed at temperatures of 650 and 750 °C compared to films annealed at 550 °C. Considering the minimum crack resistance of such films in a stressed state and the transcrystalline nature

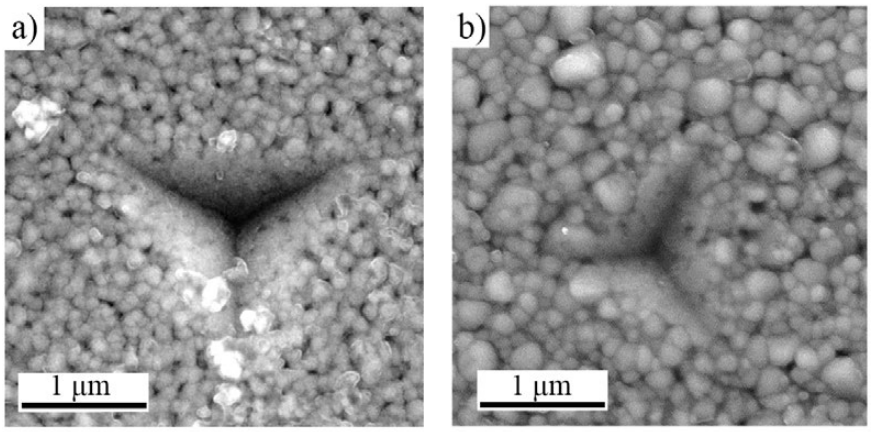

Fig. 7. SEM images of indenter imprints on the surface of films grown on a (0001) LN single crystal, annealed at 750 (a) and 800°C (b), with an indenter load of 10 mN

Table 4. Mechanical properties of lithium niobate

Substrate: Si/SiO_2						
Temperature TA, °C	–	550	650	750	800	850
H, hPa	4.6	7.4	6.0	6.7	8.1	5.0
E, hPa	80.8	118.2	119.5	124.0	129.4	112.7
η, %	31	38	34	35	36	30
Substrate: surface (0001) of LN single crystal						
Temperature TA, °C	–	550	650	750	800	850
H, hPa	6.2	10.3	9.3	7.9	7.7	6.9
E, hPa	115.5	144.5	155.0	154.1	128.3	134.7
η, %	30	48	36	37	42	38
Single crystal LN (0001)						
H, hPa	8,5					
E, hPa	157					
η, %	43					

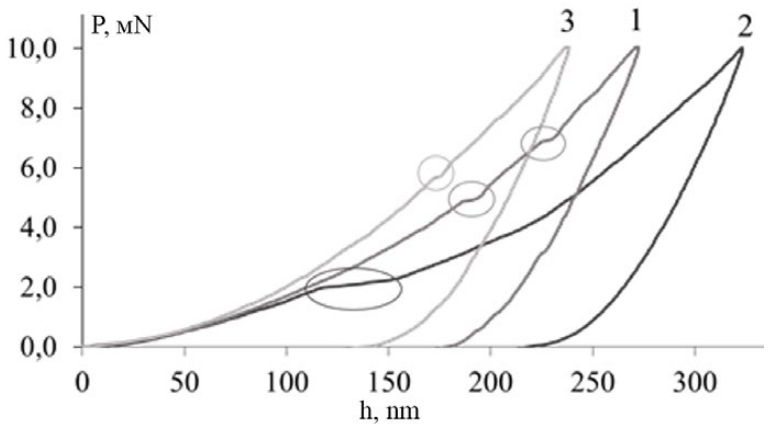

Fig. 8. *P-h* diagrams obtained from the results of indentation of the Li-Nb-O/SiO2/Si heterostructure after annealing at 550 (1) and 850°C (2) and of the surface (0001) LN single crystal (3); indenter load 10 mN

of their cracking, it is possible to assume a relationship between their strength properties and a structural feature: the greatest correspondence of the lattice parameters to single-crystal stoichiometric LN. This correspondence is probably due to the minimum content of point defects (primarily oxygen vacancies) inside the crystallites among the obtained films. This feature of the substructure leads to increased dislocation mobility and intragranular plasticity, which, combined with a minimum amount of impurities at the grain boundaries, contributes to the transcrystalline nature of crack propagation. In [20], it was shown that the scratching depth at which no crack formation was observed in a lithium niobate single crystal was 40 nm. The indentation depth of the same order for our films corresponded to a load on the indenter of 1 mN. That is, in films annealed at 750 °C, the conditions for crack formation are similar to those for a single crystal. A further increase in the TA temperature leads to saturation of the boundaries with excess oxygen, weakening the intergranular bonds and promoting crack propagation mainly along the boundaries.

The Young's modulus (E) of LN films on the surface of (0001) LN single crystal after TA at 550–750 °C (with the greatest correspondence of lattice parameters to the single crystal) was closest to the value of E for the single crystal. The hardness of crystalline films on the surface of LN single crystal was maximal in the case

of a fine-grained structure, exceeding the hardness of the single crystal, and decreased with increasing temperature. The observed dependence of hardness, considering the absence of macrostresses in the films, was characteristic of materials with a dislocation mechanism of plastic deformation and corresponds to the Hall-Petch relationship [21].

Fig. 9 shows AFM images of indenter imprints on the surface of films grown on SiO_2/Si, and profilograms in directions corresponding to the height (X1) and the center line (X2) of the triangular indenter imprint in the film plane. The indenter penetration depth is up to 200 nm, which is an order of magnitude greater than the roughness and four times less than the thickness of the tested film. The angle between the face and the opposite edge in the used indenter is 142°. Consequently, the aperture angle of the profilogram in the X1 direction will be 142° under the condition of absolute plasticity of the material. Considering elastic recovery, this angle will be slightly larger. Based on the geometry of the indenter, the left and right parts of the imprint profile in the X2 direction are absolutely symmetrical. It was found that the profiles of imprints in the X1 direction had an aperture angle of 154°, 152°, and 146° in films after annealing at 550, 750, and 800 °C, respectively (see Table 5). As can be seen from Table 5, in films after annealing at 550 °C, elastic recovery occurred equally in all directions. In contrast, in the film after annealing at 750 and 800 °C, the most significant elastic recovery occurred where the deforming effect was exerted by the indenter face, and not by the edge. This indicates a lower elasticity of the films annealed at higher temperatures, as well as the initiation of brittle fracture of the film by the indenter edges. The profiles of the imprints in the X2 direction do not differ, since the NI process does not cause brittle fractures of the film in this direction. As a result of indentation, heaping is formed at the edges of the imprints (Fig. 9). The surface of the heaping retains relief elements corresponding to the initial surface of the sample. According to SEM data, the relief elements inside the imprint also correspond to the initial surface (Figs. 6, 7). The observed relief indicates that plastic deformation was partially caused by the mechanism of intergranular sliding [19, 22]. In the most dispersed films, this mechanism is obviously dominant.

4. Conclusion

Thus, thermal annealing in an oxygen-containing atmosphere at a temperature of

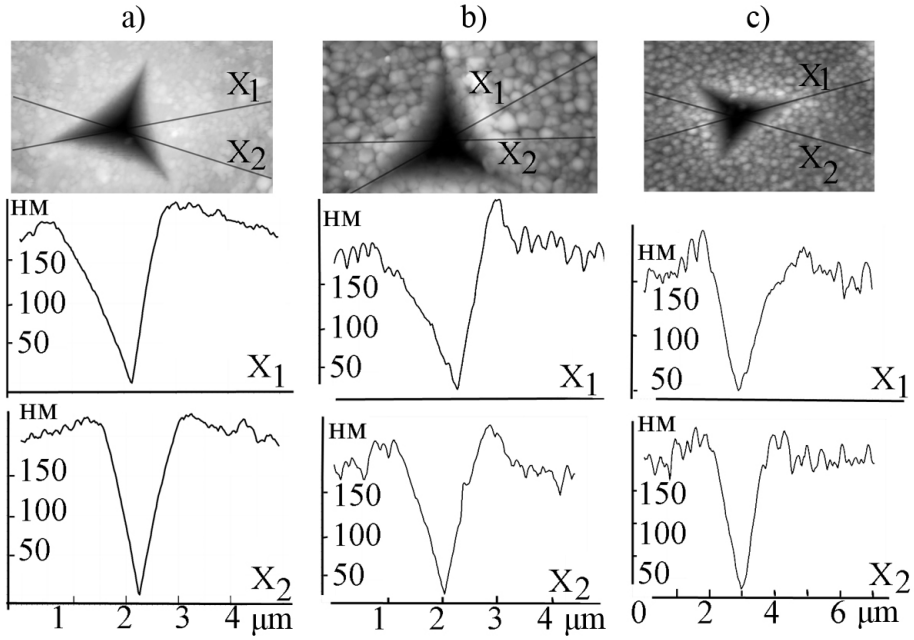

Fig. 9. AFM images of indenter imprints on the surface of films annealed at 550 (a), 750 (b), and 800 °C (c) and the corresponding profilograms in the X1 and X2 directions; indenter load 10 mN

Table 5. Geometry of the indenter imprint according to AFM data

Temperature TA, °C	550		750		800		Indenter angles	
Profile direction	X_1	X_2	X_1	X_2	X_1	X_2	X_1	X_2
Print Profile Angles, °	7	16	8	17	14	16	14	20
	154	148	**152**	146	**146**	148	**142**	135
	19	16	20	17	20	16	26	20

550-850 °C induces the crystallization of quasi-amorphous Li-Nb-O layers and the synthesis of single-phase LN films with a LN lattice. The lattice parameters of the films approach the parameters of single-crystal LN of a stoichiometric composition with increasing temperature. During the deformation of Li-Nb-O films, the most probable mechanisms are: brittle fractures, plastic deformation of crystallites, and grain boundary sliding. LN films synthesized at a temperature of 650–750 °C are most prone to brittle fractures. Brittle fractures occur due to the buildup of macrostresses in the films, resulting from different coefficients of thermal expansion of the film and the substrate. The crack resistance of the films increases significantly when using a substrate with a CTE close to that of the film. The hardness of nano- and microcrystalline LN films is always higher than the hardness of quasi-amorphous Li-Nb-O composition films. The decrease in the hardness of films synthesized at a high annealing temperature is due to a decrease in the concentration of point defects and an increase in the size of the crystallites.

Contribution of the authors

The authors contributed equally to this article.

Conflict of interests

The authors declare that they have no known competing financial interests or personal relationships that could have influenced the work reported in this paper.

References

1. Huang C. H. J., Rabson T. A. Low-loss thin-film $LiNbO_3$ optical waveguide sputtered onto a SiO_2/Si substrate. *Optics Letters*. 1993;18(10): 811–813. https://doi.org/10.1364/OL.18.000811

2. Xu H., Dong S., Xuan W., … Luo J. Flexible surface acoustic wave strain sensor based on single crystalline $LiNbO_3$ thin film. *Applied Physics Letters.* 2018;112: 093502. https://doi.org/10.1063/1.5021663

3. Jiang H., Dai C., Shen B., Jun J. High-performance $LiNbO_3$ domain wall memory devices with enhanced selectivity via optimized metal–semiconductor contact. *Nanomaterials*. 2024;14(12): 1031. https://doi.org/10.3390/nano14121031

4. He J., Ye Z. Highly C-axis oriented $LiNbO_3$ thin film on amorphous SiO_2 buffer layer and its growth mechanism *Chinese Science Bulletin*. 2003;48: 2290–2294. https://doi.org/10.1360/03ww0053

5. Maurel A., Mercier J.-F., Lund F. Lund scattering of an elastic wave by a single dislocation. *The Journal of the Acoustical Society of America*. 2004;115(6): 2773–2780. https://doi: 10.1121/1.1687735

6. Hewig G. M., Jain K., Sequeda F. O., Tom R., Wang P.-W. Sputtering of $LiNbO_3$. *Thin Films Thin Solid Films*. 1982;88: 67–74. https://doi.org/10.1016/0040-6090(82)90351-0

7. Paldi R. L., Qi Z., Misra S., … Wang H. Nanocomposite-seeded epitaxial growth of single-domain lithium niobate thin films for surface acoustic wave devices. *Advanced Photonics Research*. 2021;2: 2000149. https://doi.org/10.1002/adpr.202000149

8. Ievlev, V. M., Belonogov E. K., Dybov V. A., … Sumets M. P. Synthesis of lithium niobate during crystallization of amorphous Li–Nb–O film. *Inorganic Materials*. 2019;55(12): 1237–1241. https://doi.org/10.1134/S0020168519120069

9. Shandilya S., Tomar M., Gupta V. Deposition of stress free c-axis oriented $LiNbO_3$ thin film grown on (002) ZnO coated Si substrate. *Journal of Applied Physics*. 2012;111: 10–16. https://doi.org/10.1063/1.4714664

10. Fakhri M. A., Salim E. T., Hashim U., Abdulwahhab A. W., Salim Z. T. Annealing temperature effect on structural and morphological properties of nano photonic $LiNbO_3$. *Journal of Materials Science: Materials in Electronics*. 2017;28: 16728–16735. https://doi.org/10.1007/s10854-017-7586-y

11. Zhu N., Chen J., Zhou P., Zhu Y. Effect of the anisotropy mechanical properties on LN crystals fixed-abrasive lapping *Materialsю* 2020;13(19): 4455. https://doi.org/10.3390/ma13194455

12. Fries E., Péter A. Plastic deformation of $LiNbO_3$ single crystalsю *Revue de Physique Appliquée*. 1987;22(11): 1353–1359. https://doi.org/10.1051/rphysap:0198700220110135300

13. Péter Á., Fries E., Rivière J. P. TEM observation of plastically induced dislocations in lithium niobate $LiNbO_3$ single crystals. *Physica Status Solidi (a)*. 1991;128(1): 45–53. https://doi.org/10.1002/pssa.2211280106

14. Xie H., Lu Y.-C., Raj R. Transmission electron microscopy study of microstructure and misfit dislocations in epitaxial $LiTaO_3$ thin films grown on sapphire by a metalorganic chemical vapor deposition process *Journal of Applied Physics*. 1996;79(7): 3675–3680. https://doi.org/10.1063/1.361197

15. Veignant F., Gandais M., Aubert P., Guy G. Epitaxial growth of $LiNbO_3$ on αAl_2O_3 (0001). *Thin Solid Films*. 1998;336:(1-2): 163–167. https://doi.org/10.1016/S0040-6090(98)01222-X

16. Bartasyte A., Plausinaitiene V., Abrutis A., … Saltyte Z. Residual stresses and clamped thermal expansion in $LiNbO_3$ and $LiTaO_3$ thin films. *Applied Physics Letters*. 2012;101: 122902. https://doi.org/10.1063/1.4752448

17. Иевлев В. М., Канныкин С. В., Костюченко А. В., Белоногов Е. К., Путляев В. И. Об информативности рентгеновских дифрактограмм в виде гало. *Неорганические Материалы*. 2020:56(8): 906–913. https://doi.org/10.31857/s0002337x20080059

18. Shiozaki Y., Mitsui T. Powder neutron diffraction study of $LiNbO_3$. *Journal of Physics and Chemistry of Solids*. 1963;24: 1057–1061. https://doi.org/10.1016/0022-3697(63)90012-x

19. Ievlev V. M., Kostyuchenko A. V., Darinskii B. M., Barinov S. M. Hardness and microplasticity of nanocrystalline and amorphous calcium phosphate coatings. *Physics of the Solid State*. 2014;56(2): 321–329. https://doi.org/10.1134/s1063783414020127

20. Nakamura M., Fujiyama H., Sumomogi T. Effects of material properties on ductile mode machining in ultra-precision grinding of lithium niobate. *Hiroshima International University Research Report*. 2012;45: 11–20. Available at: https://xueshu.baidu.com/usercenter/paper/show?paperid=a25d14fe8a5e8d01a7d1aad2ec1c522e

21. Hall E. O. Variation of hardness of metals with grain size. *Nature*. 1954;173: 948–949. https://doi.org/10.1038/173948b0

22. Kim B.-N., Hiraga K., Sakka Y., Ahn B.-W. A grain-boundary diffusion model of dynamic grain growth during superplastic deformation. *Acta Materialia*. 1999;47(12): 3433–3439. https://doi.org/10.1016/s1359-6454(99)00201-3

Information about the authors

Aleksandr V. Kostyuchenko, Cand. Sci. (Phys.–Math.), Associate Professor, Department of Solid State Electronics, Voronezh State Technical University (Voronezh, Russian Federation).
http://orcid.org/0000-0002-0049-3664
av-kostuchenko@mail.ru

Evgeny K. Belonogov, Dr. Sci. (Phys.–Math.), Professor, Department of Physics, Voronezh State Technical University (Voronezh, Russian Federation).
http://orcid.org/0000-0002-0216-0986
ekbelonogov@mail.ru

Valentin M. Ievlev, Full Member of the Russian Academy of Sciences, Dr. Sci. (Phys.–Math.), Professor, Head of the Department of Interdisciplinary Materials Science, Lomonosov Moscow State University (Moscow, Russian Federation).
http://orcid.org/0000-0002-3205-2580
rnileme@mail.ru

Alexander E. Nikonov, Cand. Sci. (Phys.–Math.), Researcher of the Functional Materials Laboratory, Voronezh State Technical University (Voronezh, Russian Federation).
http://orcid.org/ 0009-0000-0852-2303
nikonov.sasha1994@gmail.com

Evgeny A. Osipov, student, Department of Solid State Electronics, Voronezh State Technical University (Voronezh, Russian Federation).
http://orcid.org/0009-0002-1209-3833
sanr1ze1@mail.ru

Pavel A. Osipov, student, Department of Solid State Electronics, Voronezh State Technical University (Voronezh, Russian Federation).
http://orcid.org/ 0009-0003-3891-2646
rejmefun@mail.ru

Received December 11, 2024; approved after reviewing June 18, 2025; accepted for publication July 15, 2025; published online September 25, 2025.